Video Article

Experimental Methods of Dust Charging and Mobilization on Surfaces with Exposure to Ultraviolet Radiation or Plasmas

Xu Wang[1,2], Joseph Schwan[1,2], Noah Hood[1,2], Hsiang-Wen Hsu[1,2], Eberhard Grün[1,2], Mihály Horányi[1,2]

[1]Laboratory for Atmospheric and Space Physics, University of Colorado

[2]NASA/SSERVI's Institute for Modeling Plasma, Atmospheres and Cosmic Dust

Correspondence to: Xu Wang at xu.wang@colorado.edu

URL: https://www.jove.com/video/57072
DOI: doi:10.3791/57072

Keywords: Environmental Sciences, Issue 134, Dust charging, electrostatic dust transport, dusty plasma, photoelectrons, secondary electrons, regolith, airless bodies, Moon, asteroids, surface processes

Date Published: 4/3/2018

Citation: Wang, X., Schwan, J., Hood, N., Hsu, H.W., Grün, E., Horányi, M. Experimental Methods of Dust Charging and Mobilization on Surfaces with Exposure to Ultraviolet Radiation or Plasmas. *J. Vis. Exp.* (134), e57072, doi:10.3791/57072 (2018).

Abstract

Electrostatic dust transport has been hypothesized to explain a number of observations of unusual planetary phenomena. Here, it is demonstrated using three recently developed experiments in which dust particles are exposed to thermal plasma with beam electrons, beam electrons only, or ultraviolet (UV) radiation only. The UV light source has a narrow bandwidth in wavelength centered at 172 nm. The beam electrons with the energy of 120 eV are created with a negatively biased hot filament. When the vacuum chamber is filled with the argon gas, a thermal plasma is created in addition to the electron beam. Insulating dust particles of a few tens of microns in diameter are used in the experiments. Dust particles are recorded to be lofted to a height up to a few centimeters with a launch speed up to 1 m/s. These experiments demonstrate that photo and/or secondary electron emission from a dusty surface changes the charging mechanism of dust particles. According to the recently developed "patched charge model", the emitted electrons can be re-absorbed inside microcavities between neighboring dust particles below the surface, causing the accumulation of enhanced negative charges on the surrounding dust particles. The repulsive forces between these negatively charged particles may be large enough to mobilize and lift them off the surface. These experiments present the advanced understanding of dust charging and transport on dusty surfaces, and laid a foundation for future investigations of its role in the surface evolution of airless planetary bodies.

Video Link

The video component of this article can be found at https://www.jove.com/video/57072/

Introduction

Airless planetary bodies, such as the Moon and asteroids, are covered with fine dust particles called regolith. These airless bodies, unlike Earth, are directly exposed to solar wind plasma and solar ultraviolet (UV) radiation, causing the regolith dust to be charged. These charged dust particles may therefore be mobilized, lofted, transported, or even ejected and lost from the surface due to electrostatic forces. The first suggested evidence of this electrostatic process was the so-called "lunar horizon glow", a distinct glow above the western horizon observed shortly after sunset by Surveyor 5, 6, and 7 spacecraft five decades ago (**Figure 1a**)[1,2,3]. It has been hypothesized that this glow was caused by sunlight scattered off from electrostatically lofted dust particles (5 μm radius) to a height < 1 m above the surface near the lunar terminator[1,2,3]. Electrostatically released fine dust was also suggested to be responsible for the ray-like streamers reaching a high altitude reported by the Apollo astronauts[4,5].

Ever since these Apollo observations, a number of observations over other airless bodies were also linked to the mechanisms of electrostatic dust mobilization or lofting, such as the radial spokes in the Saturn's rings[6,7,8], the dust ponds on asteroid Eros (**Figure 1b**)[9] and comet 67P[10], the porous surfaces indicated from the main-belt asteroid spectra[11], the unusually smooth surface of Saturn's icy moon Atlas[12], and the regolith at the lunar swirls[13]. In addition, the degradation of the laser retroreflectors on the lunar surface may be also caused by the accumulation of electrostatically lofted dust[14].

Laboratory studies have been largely motivated by these unusual space observations in order to understand the physical processes of dust charging and transport. Dust mobilization has been observed in various plasma conditions, in which dust particles are shed off from a glass sphere surface[15,16], levitated in plasma sheaths[17], and recorded to move on both conducting and insulating surfaces[18,19,20,21]. However, how dust particles gain large enough charges to be lofted or mobilized remained poorly understood. The measurements of the charges on individual dust particles on a smooth surface[22] and the average charge density on a dusty surface[23] immersed in plasmas show that the charges are far too small for dust particles to be lofted or mobilized.

In the prior theories[16,24,25], the charging was only considered to occur on the top surface layer that is directly exposed to UV or plasma. Charges are often considered to be distributed uniformly over the entire dusty surface, *i.e.*, each individual dust particle acquires the same amount of charge, described by the so-called "shared charge model"[16]. However, the charges calculated from this model are much smaller than

the gravitational force alone. A charge fluctuation theory that accounts for the stochastic process of the fluxes of electrons and ions to the surface[16,24] shows a temporal enhancement in the electrostatic force, but it remains small in comparison to the gravitational force.

In this paper, electrostatic dust lofting and mobilization is demonstrated using three recently developed experiments[26], which are important for understanding dust transport on the regolith of airless planetary bodies. These experiments are performed in the conditions of thermal plasma with beam electrons, beam electrons only or UV radiation only. These experiments demonstrate the validity of the recently developed "patched charge model"[26,27], in which microcavities formed between neighboring dust particles below the surface can re-absorb the emitted photo and/or secondary electrons, generating large negative charges on the surfaces of the neighboring dust particles. The repulsive forces between these negative charges can become large enough to mobilize or lift off the dust particles.

Protocol

1. Vacuum chamber setup

1. Place an insulating rubber sheet (0.2 cm thick, 5 cm in diameter) with a central hole 1.9 cm in diameter on an insulating plate (2 cm thick and 20 cm in diameter) (**Figure 2a, b**). Load insulating, irregularly-shaped dust particles (between 10 and 50 μm in diameter) in the hole.
2. Place the insulating plate on a metal plate standing in the middle of a vacuum chamber. Electrically isolate the metal plate from the chamber using ceramic standoffs.
3. Turn on the vacuum pumps (a turbo pump backed by a mechanical roughing pump) to reach the base pressure of ~ 10^{-6} Torr. The demonstrating experiments are performed in a cylindrical stainless-steel vacuum chamber, 50 cm in diameter and 28 cm tall (**Figure 2c**).
4. Record the dust movement and lofting with a video camera at a regular speed of 30 frames/s (fps) or a high-speed (> 2000 fps) camera. Use an LED light with the maximum illumination equivalent to > 500W incandesce light to produce enough lighting on the dust particles for good-quality video recording.
   NOTE: Using the rubber is because of its dark color that minimizes the light reflection to the camera. Light-colored dust particles should be used for better photographing due to the color contrast to the dark rubber surface. The thick insulating plate is used for eliminating the effect of the electric field between the surface of the insulating plate and metal plate on the dust charging and mobilization. In this demonstration, Mars simulant (JSC-Mars-1, sieved to the mean diameter of 38-48 μm, mass density of 1.9 g/cm^{-3} and major composition of SiO_2 [28]) were used, which resembles the general regolith dust of airless bodies in the inner solar system. Various other types of insulating dust particles were also tested, such as lunar simulant (JSC-1), lunar simulant highland (LHT) and pure silica dust.

2. Exposure to thermal plasma with beam electrons

1. Attach a thoriated tungsten filament (0.1 mm thick and ~ 3 cm long) to an electrode feedthrough and install it on the top of the chamber. Then pump the chamber down to the base pressure.
2. Fill the vacuum chamber with argon gas to the pressure of ~ 0.5 mTorr.
3. Turn on the power supplies and set the bias voltage -120 V to the filament.
4. Increase the heating voltage to the heating current ~ 2A until the emission current reaches a desired value (a few mA). Energetic electrons with the energy of 120 eV will be emitted from the filament.
   NOTE: These beam-like primary electrons impact neutral argon atoms, causing them to be ionized and creating a plasma with an electron temperature around 2 eV. A large fraction of the primary beam electrons directly reaches the dusty surface without collisions with neutral atoms. Dust particles are therefore exposed to both the thermal plasma and beam electrons.
5. To show the role of energetic beam electrons in dust transport, use an alternative operation of creating a thermal plasma above dust particles.
   1. Turn on an alternative filament in the bottom of the chamber with the bias voltage -40 V and emission current up to 400 mA (**Figure 2a**). The primary electrons emitted from the filament will be stopped by the metal plate below the insulting plate on which the dust particles rest (**Figure 2a, b**).
   2. Vary the emission current to change the electric field above the surface. Higher current creates higher plasma density, thinner sheath, and thus larger electric field.

3. Exposure to beam electrons only

1. Setup the experiment as described in the above experiment using the top filament.
2. Turn on the top filament under the base pressure 10^{-6} Torr (*i.e.*, no argon gas fed in the chamber). No plasma is created while only the 120 eV beam electrons emitted from the filament bombard the dust particles.
3. Operate the filament in two different modes.
   1. Set the bias voltage to -120 V, then increase the heating voltage until the emission current reaches a few mA.
   2. Increase the heating voltage to reach a desired heating current ~ 2 A, then increase the bias voltage from 0 V gradually to -120 V to emit electrons with an emission current of a few mA.

4. Exposure to UV radiation only

1. Replace the top filament with a UV lamp (**Figure 2b**) and pump down the chamber to the base pressure. Use a xenon excimer Osram lamp, which emits the UV light of 172 nm wavelength. The corresponding photon energy is 7.2 eV, larger than the work function of the dust surface (~ 5.5 eV) in order to emit photoelectrons.
   NOTE: Shorter wavelength UV that radiates higher energy photons is expected to create more charges on the dust particles and therefore more mobilization, based on the patched charge model[26,27].

2. Turn on the UV lamp to radiate dust particles. In the demonstration, the photon irradiance is 40 mW/cm^{-2} at the UV source and ~ 16 mW/cm^{-2} at the dusty surface.

Representative Results

A set of experiments were performed using the top or bottom filaments. With the top filament setup, the hopping of the dust particles was recorded (**Figure 3a**). In contrast, the dust particles remained at rest when using the bottom filament. It has been measured that the vertical electric field at the surface was approximately same (16 V/cm) in both experiments under the conditions described in Protocol step 2[26]. These results indicate that the electrostatic force due to the sheath electric field is not large enough to mobilize dust particles. The only difference between these two experiments is the presence (using the top filament) or absence (using the bottom filament) of beam electrons bombarding the surface.

Potentials across the dust and outside rubber surfaces measured by Wang *et al.*[26] have shown that secondary electrons were generated due to the bombardment of the energetic beam electrons while minimized in the plasma in which the electrons are thermalized. More importantly, these potential measurements have shown that the secondary electron emission was largely reduced on the dusty surface, comparing to that on the solid surface[26]. This is likely due to the surface roughness that can re-absorb the emitted electrons[20,29,30,31,32,33].

As described in Protocol 3.3.1, secondary electrons are created once the 120 eV beam electrons emitted from the filament reach the surface, causing the surface potential to rise to become more positive than -120 V. In this case, the dust particles were mobilized and lofted from the surface (**Figure 3b**). In 3.3.2, no dust movement was recorded. It has been measured that the surface potential simply follows the filament bias voltage to become -120 V[26]. This is because the filament voltage starts very small, *i.e.*, the corresponding beam electron energy is very low, and the secondary electron yield is nearly zero so the surface potential equals to the energy of the beam electrons (in eV) to stop them to maintain a zero-net current at the equilibrium state. The increment of the filament voltage is gradual, compared to the plasma response, so that the voltage increment is too small to create any secondary electrons. Therefore, the surface potential follows the filament voltage, causing the beam electrons to be stopped from reaching the surface and therefore suppressing the secondary electron emission. Again, this experiment shows that the generation of secondary electrons significantly contributes to the dust charging and transport process.

The dust hopping was recorded under the 172 nm UV radiation (**Figure 3c**). A photoelectron sheath is created above the surface, in which the electric field is very small ~ 0.5 V/cm[34]. The electrostatic force due to the sheath electric field is therefore negligible. As shown by Schwan *et al.*[27], lofted dust particles under UV radiation carry large negative charges. This result contradicts the expected positive charge due to photoemission while is in agreement with the "patched charge model" described below.

Long exposure of the dust particles under the UV radiation was also performed. **Figure 4** shows the changes in the surface morphology as a function of time. The surface becomes smoother and eventually flattens out, offering an efficient process for the dust ponds formed on asteroid Eros (**Figure 1b**), for example.

The three experiments demonstrated above show that dust lofting occurs when photo and/or secondary electrons are emitted from a dusty surface, and these emitted electrons can be re-absorbed within the surface due to its roughness. The "patched charge model" developed by Wang *et al.*[26] was based on these two findings and is briefly reviewed below.

As shown in **Figure 5**, contrary to a smooth solid surface, microcavities are formed between dust particles below a regolith surface. The top surfaces (blue patches) are charged by photoionization due to UV radiation and/or plasma electrons and ions. There are small openings between dust particles on the top surface. Some of the UV photons, or electrons and ions can penetrate through these small openings onto the dust particles below the top surface, creating photoelectrons and/or secondary electrons. Many of these emitted electrons do not escape and are re-absorbed inside the microcavity and deposit negative charges on the surfaces of the surrounding particles (red patches).

The charge on the blue surface patches is $Q_b \propto E_b$, where E_b is the sheath electric field above the dusty surface. The red patches are charged to $Q_r \propto E_r$, where E_r is the electric field inside the microcavity. $E_b \propto 1/\lambda_{De}$, where λ_{De} is the Debye length while $E_r \propto 1/r$, where r is the individual dust particle radius, approximately similar to the characteristic size of the microcavity. Because of $\lambda_{De} >> r$, $E_r >> E_b$ and therefore $Q_r >> Q_b$. The largely enhanced negative charge Q_r may create a large enough repulsive force between two negatively charged particles, which ejects them off the surface. Large charge deposits (on the order of 0.5 μC/m^2) within a dusty surface due to re-absorption of photoelectrons are also observed in a computer simulation[35].

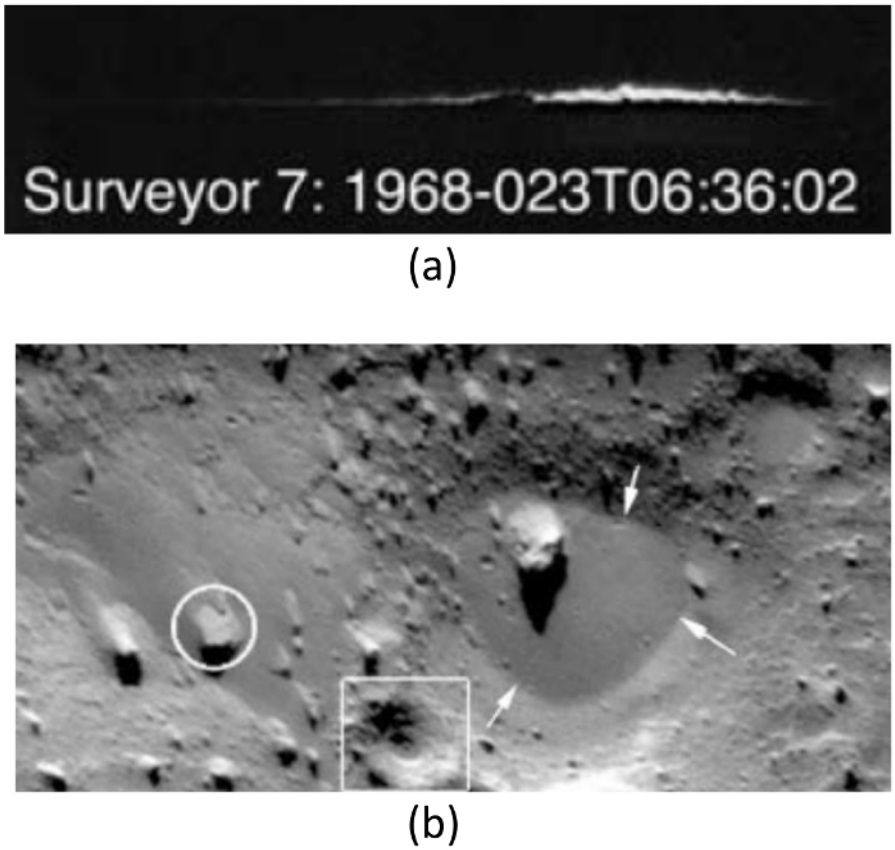

Figure 1. Photos of two examples of the unusual surface phenomena related to electrostatic dust transport. (a) The lunar horizon glow taken by Surveyor 7 spacecraft[3] (NASA Photo). (b) Fine dust deposits in a crater, the so-called "dust pond" on asteroid 433 Eros taken by the NEAR-Shoemaker spacecraft[9]. Arrows and circle indicate pre-existing toporgraphies. Square highlights a small isolated dust pond. Please click here to view a larger version of this figure.

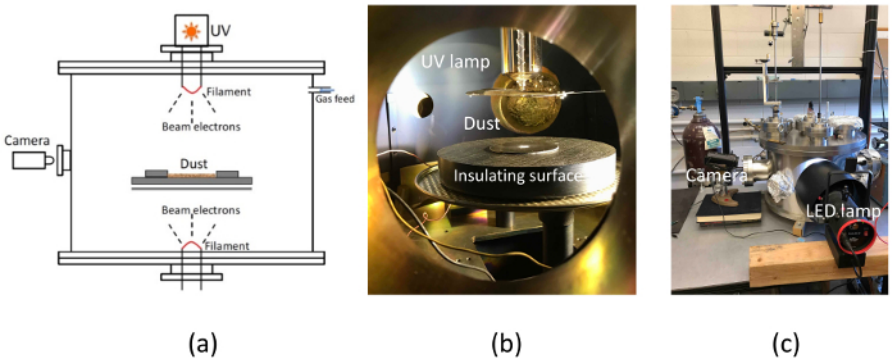

Figure 2. Experimental apparatus and setup. (a) Schematic of the experimental setup for dust exposure to a thermal plasma with beam electrons, beam electrons only or UV radiation only[26]. (b) Picture showing the setup for the UV experiment inside the chamber and (c) picture of the vacuum chamber. Please click here to view a larger version of this figure.

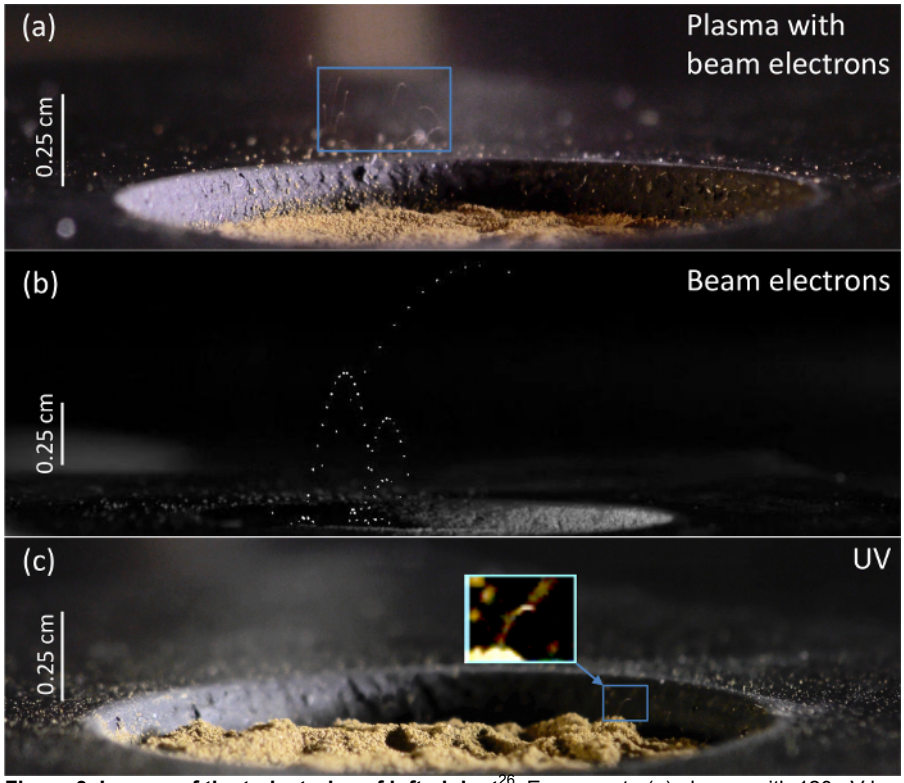

Figure 3. Images of the trajectories of lofted dust[26]. Exposure to (a) plasma with 120 eV beam electrons, (b) 120 eV beam electrons, and (c) UV radiation, respectively. A blue box in (a) highlights the trajectories of the lofted dust particles. A blue box in (c) highlights the trajectory of a lofted dust particle with a zoomed view. The lofted dust particles include aggregates as large as 140 m in diameter besides individual particles (38 - 45 m in diameter). This figure has been modified from the paper by Wang *et al.*[26]. Please click here to view a larger version of this figure.

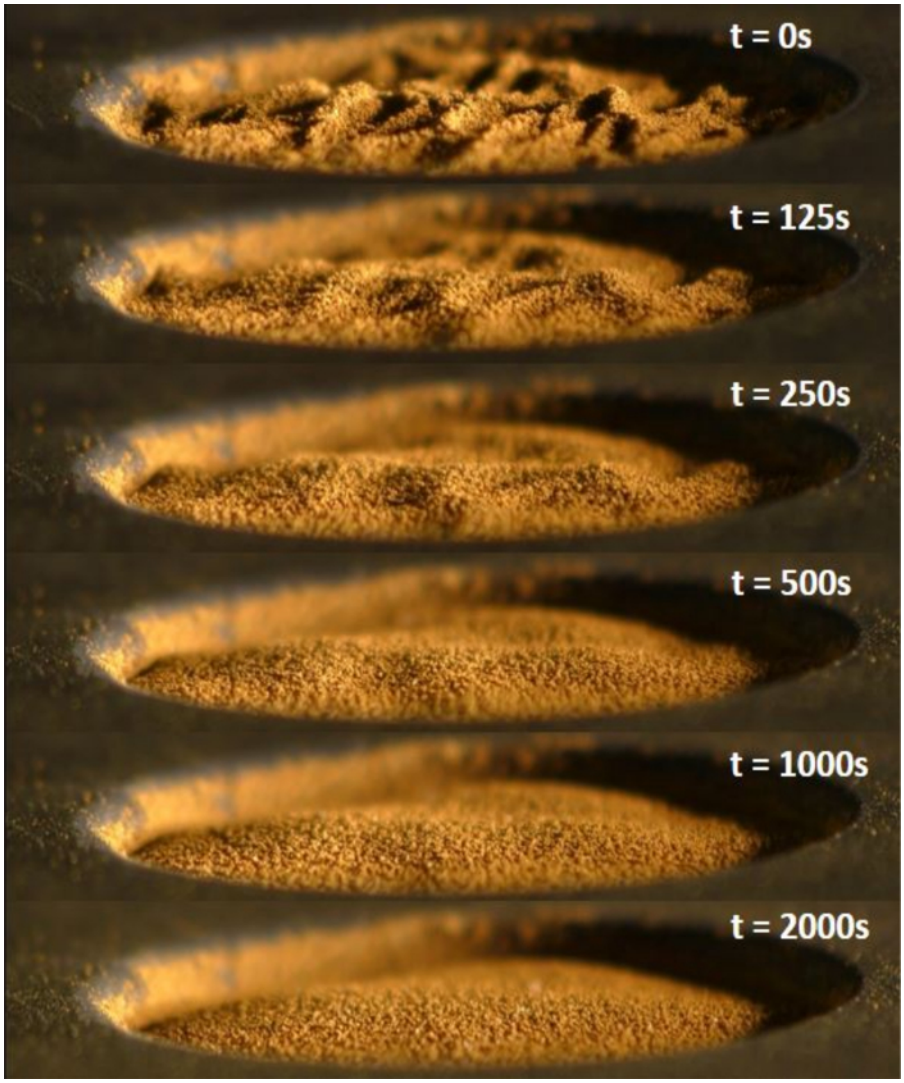

Figure 4. Time lapse of the surface change due to the dust moblization under the UV radiation. The UV wavelength is 172 nm with the photon irradiance of 16 mW/cm^2 at the dusty surface. Please click here to view a larger version of this figure.

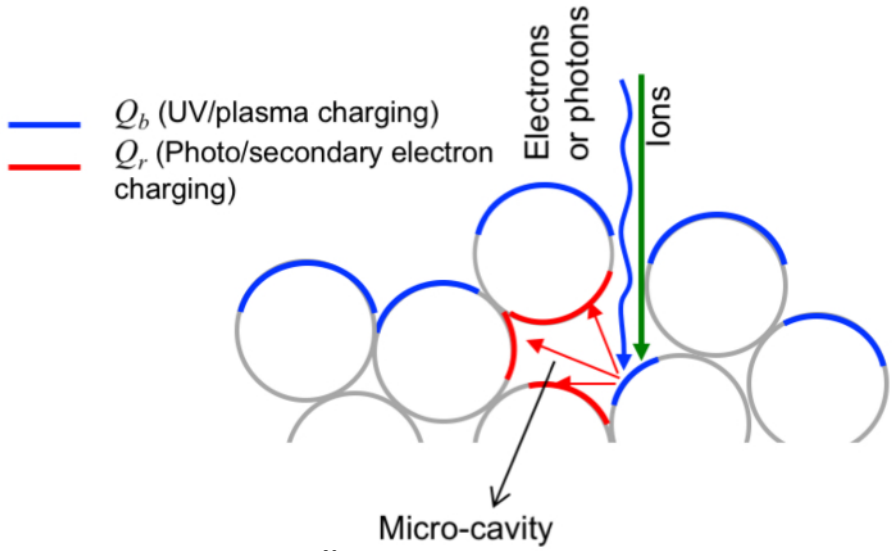

Figure 5. Patched charge model[26]. A microcavity shown in the center is formed by neighboring dust particles (grey circles). The blue surface patches are exposed to photons and/or electrons and ions. They are charged to Q_b and simultanously emit photo and/or secondary electrons. A fraction of these emitted electrons are re-absorbed inside the microcavity and accumulate on the red surface patches of the surrounding dust particles, charging them negatively to Q_r. Please click here to view a larger version of this figure.

Discussion

For decades, the problem of electrostatic dust transport on the regolith of airless bodies remained an open question how regolith dust particles gain sufficiently large charges to become mobilized or lofted. Recent laboratory studies[26,27] have fundamentally advanced the understanding of this problem.

Here, it is demonstrated three recently developed experiments to show dust charging and mobilization in thermal plasma with beam electrons, beam electrons only or UV radiation only. The key element in these experiments is to create secondary electrons or photoelectrons to be emitted from dusty surfaces. As shown in the previous work[26], it is likely that these emitted electrons can result in largely enhanced negative charges on the dust particles due to their re-absorption inside the microcavities below the dusty surface. The detailed mechanism is described with the recently developed and successfully verified "patched charge model" [26,27].

In Protocol step 1 and 2, dust particles need to be directly exposed to beam electrons with energies above 100 eV to create secondary electrons efficiently[36]. The bias voltage to the filament should be set first, then increasing the heating voltage until the desired emission current is reached, as described in Protocol 3.3.1. If dust particles are not moved or lofted, it may indicate the dust surface potential follows the beam energy to become so negative that the creation of secondary electrons is suppressed. This can be caused by a wrong operation on setting the filament voltages, as described in Protocol 3.3.2.

In Protocol step 3, the wavelength of the UV lamp should be 170 nm or shorter so that the energies of UV photons are significantly larger than the work function of the dust surface in order to emit photoelectrons efficiently. Dust mobilization largely depends on the cohesive forces between dust particles, which may vary with different compositions. Mars simulant was shown to be the easiest to move.

These experiments show that dust particles (tens of microns in diameter) can jump up to a few centimeters high. This height is equivalent to tens of centimeters on the Moon surface, similar to the height of the lunar horizon glow. It is not clear whether the glow is caused by the ballistic hopping or levitation of dust particles. These experiments suggest that the former one is a more likely mechanism. It was shown that electrostatic dust mobilization can lead to the formation of smooth surfaces, which may be relevant to the dust ponds formed on asteroid Eros[9] and comet 67P[10], and the highly smooth surface of Saturn's icy moon Atlas[12].

In conclusion, these experiments show that electrostatic dust transport is expected to play a significant role in shaping the surfaces of airless planetary bodies and may be responsible for a number of unusual surface phenomena. The methods demonstrated here opened a door for more advanced studies including both laboratory experiment and modeling in the future.

Disclosures

The authors have nothing to disclose.

Acknowledgements

This work was supported by the NASA/SSERVI's Institute for Modeling Plasma, Atmospheres and Cosmic Dust (IMPACT) and by the NASA Solar Systems Workings Program (Grant number: NNX16AO81G).

References

1. Criswell, D. R. "Horizon-glow and the motion of lunar dust" in *Photon and Particle Interactions with Surfaces in Space*. (Springer, New York), pp. 545-556 (1973).
2. Rennilson, J. J., Criswell, D. R. Surveyor observations of lunar horizon-glow. *Moon.* **10** (2), 121-142 (1974).
3. Colwell, J.E., Batiste, S., Horányi, M., Robertson, S., Sture, S. Lunar surface: Dust dynamics and regolith mechanics. *Rev. Geophys.* **45**, RG2006 (2007).
4. McCoy, J. E., Criswell, D. R. Evidence for a high latitude distribution of lunar dust. *The 5th Proc. Lunar Sci. Conf.* 2991 (1974).
5. Zook, H. A., McCoy, J. E. Large scale lunar horizon glow and a high altitude lunar dust exosphere. *Geophys. Res. Lett.* **18** (11), 2117-2120 (1991).
6. Smith, B. A. *et al.* Encounter with Saturn - Voyager-1 imaging science results. *Science.* **212** (4491), 163-191 (1981).
7. Smith, B. A. *et al.* A new look at the Saturn system - the Voyager-2 images. *Science.* **215** (4532), 504-537 (1982).
8. Mitchell, C. J., Horányi, M., Havnes, O., Porco, C. C. Saturn's spokes: Lost and found. *Science.* **311** (5767), 1587-1589 (2006).
9. Robinson, M.S., Thomas, P.C., Veverka, J., Murchie, S., Carcich, B. The nature of ponded deposits on Eros. *Nature.* **413** (6854), 396-400 (2001).
10. Thomas, N. *et al.* Redistribution of particles across the nucleus of comet 67P/Churyumov-Gerasimenko. *Astron. Astrophys.* **583**, A17 (2015).
11. Vernazza, P. *et al.* High surface porosity as the origin of emissivity features in asteroid spectra. *Icarus.* **221** (2), 1162-1172 (2012).
12. Hirata, N., Miyamoto, H. Dust levitation as a major resurfacing process on the surface of a saturnian icy satellite Atlas. *Icarus.* **220** (1), 106-113 (2012).
13. Garrick-Bethell, I., Head III, J. W., Pieters, C. M. Spectral properties, magnetic fields, and dust transport at lunar swirls. *Icarus.* **212** (2), 480-492 (2011).
14. Murphy, T.W. et al. Long-term degradation of optical devices on the Moon. *Icarus.* **208** (1), 31-35 (2010).
15. Sheridan, T. E., Goree, J., Chiu, Y. T., Rairden, R. L., Kiessling, J. A. Observation of dust shedding from material bodies in a plasma. *J. Geophys. Res.* **97** (A3), 2935-2942 (1992).
16. Flanagan, T. M., Goree, J. Dust release from surfaces exposed to plasma. *Phys. Plasmas* . **13** (12), 123504 (2006).
17. Sickafoose, A. A., Colwell, J. E., Horányi, M., Robertson, S. Experimental levitation of dust grains in a plasma sheath. *J. Geophys. Res.* **107**(A11), 1408 (2002).
18. Wang, X., Horányi, M., Robertson, S. Experiments on dust transport in plasma to investigate the origin of the lunar horizon glow. *J. Geophys. Res.* **114**, A05103 (2009).
19. Wang, X., Horányi, M., Robertson, S. Investigation of dust transport on the lunar surface in a laboratory plasma with an electron beam. *J. Geophys. Res.* **115**, A11102 (2010).
20. Wang, X., Horányi, M., Robertson, S. Dust transport near electron beam impact and shadow boundaries. *Planet. Space Sci.* **59** (14), 1791-1794 (2011).
21. Hartzell, C. M., Wang, X., Scheeres, D. J., Horányi, M. Experimental demonstration of the role of cohesion in electrostatic dust lofting. *Geophys. Res. Lett.* **40** (6), 1038-1042 (2013).
22. Wang, X., Horányi, M., Sternovsky, Z., Robertson, S., Morfill, G. E. A laboratory model of the lunar surface potential near boundaries between sunlit and shadowed regions. *Geophys. Res. Lett.* **34** (16), L16104 (2007).
23. Ding, N., Wang, J., Polansky, J. Measurement of dust charging on a lunar regolith simulant surface. *IEEE Trans. Plasma Sci.* **41** (12), 3498-3504 (2013).
24. Sheridan, T. E., Hayes, A. Charge fluctuations for particles on a surface exposed to plasma. *Appl. Phys. Lett.* **98** (9), 091501 (2011).
25. Heijmans, L. C. J., Nijdam, S. Dust on a surface in a plasma: A charge simulation. *Phys. Plasmas.* **23** (6), 043703 (2016).
26. Wang, X., Schwan, J., Hsu, H.-W., Grün, E., Horányi, M. Dust charging and transport on airless planetary bodies. *Geophys. Res. Lett.* **43** (12), 6103-6110 (2016).
27. Schwan, J., Wang, X., Hsu, H.-W., Grün, E., Horányi, M. The charge state of electrostatically transported dust on regolith surfaces. *Geophys. Res. Lett.* **44** (7), 3059-3065 (2017).
28. Allen, C. C., *et al.* Martian Regolith Simulant JSC-Mars-1. *The 29th Lunar and Planetary Science Conference.*, Houston, Texas. Abstract # 1690 (1998).
29. Martin, N. L. S., von Engel, A. The reflection of slow electrons from a soot-covered surface. *J. Phys DAppl Phys.* **10** (6), 863-868 (1977).
30. Halekas, J. S., Delory, G. T., Lin, R. P., Stubbs, T. J., Farrell, W. M. Lunar Prospector measurements of secondary electron emission from lunar regolith. *Planet. Space Sci.* **57** (1), 78-82 (2009).
31. Wiese, R., Sushkov, V., Kersten, H., Ikkurthi, V. R., Schneider, R., Hippler, R. Behavior of a porous particle in a radiofrequency plasma under pulsed argon ion beam bombardment. *New J. Phys.* **12**, 033036 (2010).
32. Richterová, I., Němeček, Z., Beránek, M., Šafránková, J., Pavlů, J. Secondary emission from non-spherical dust grains with rough surfaces: Applications to lunar dust. *Astrophys. J.* **761** (2), 108 (2012).
33. Ma, Q., Matthews, L. S., Land, V., Hyde, T. W. Charging of aggregate grains in astrophysical environments. *Astrophys. J.* **763** (2), 77 (2013).
34. Dove, A., Horányi, M., Wang, X., Piquette, M., Poppe, A. R., Robertson, S. Experimental study of a photoelectron sheath. *Phys. Plasmas.* **19** (4), 043502 (2012).
35. Zimmerman, M. I. *et al.* Grain-scale supercharging and breakdown on airless regoliths. *J. Geophys. Res.-Planet.* **121** (10), 2150-2165 (2016).
36. Wang, X., Pilewskie, J., Hsu, H.-W., Horányi, M. Plasma potential in the sheaths of electron-emitting surfaces in space. *Geophys. Res. Lett.* **43** (12), 525-531 (2016).

